JOURNAL OF GEOPHYSICAL RESEARCH, VOL. 105, NO. D9, PAGES 11,935–11,946, MAY 16, 2000

Interannual variability of the vertical descent rate in the Antarctic polar vortex

Nozomi Kawamoto
Department of Geophysics, Faculty of Science, Kyoto University, Kyoto, Japan

Masato Shiotani
Division of Ocean and Atmospheric Sciences, Graduate School of Environmental Earth Science
Hokkaido University, Sapporo, Japan

Abstract. To investigate a descent rate in the Antarctic polar vortex, we analyzed the long-lived trace gas data derived from the Halogen Occultation Experiment on board the Upper Atmosphere Research Satellite during the 6-year period from 1992 to 1997. By comparing the Antarctic fall (February and March) and spring (September and October) methane profiles, we estimated the middle stratospheric descent for each of the six winters. Large year-to-year variations are seen (1.2–1.8 km month^{-1} at 0.6 ppmv), which consist of a biennial oscillation and a decreasing trend for the period analyzed. The descent rate is larger in the even years (1992, 1994, and 1996) than in the odd years (1993, 1995, and 1997). Dynamical fields for the 6 years are also analyzed using the United Kingdom Meteorological Office assimilation data. The differences between the even and odd years are clear in the midwinter. In the even years the downward and poleward movement of the westerly jet occurs earlier. The thermal wind relation infers that this event is associated with the development of a "warm pool" around the Antarctic stratopause, resulting from adiabatic heating due to the downward motion of air. Planetary wave activity over the winter season is more vigorous in the even years than in the odd years, suggesting a close relationship between the mean flow and planetary waves.

1. Introduction

The first observations of sustained, unmixed vertical descent for the long-lived trace gas in the Antarctic were reported by *Russell et al.* [1993a] based on the data from the Halogen Occultation Experiment (HALOE) on board the Upper Atmosphere Research Satellite (UARS). *Schoeberl et al.* [1995] (hereinafter referred to as S95) made further refinement on estimating the descent rate using the HALOE gas data. The HALOE observes southern high latitudes (>60°S) in fall (February and March) and in spring (September and October) (see Figure 1). On the basis of 1992 spring Antarctic observation lasting about a month, S95 estimated the descent rate inside the polar vortex to be about 1.8 km month^{-1} in the lower stratosphere by tracing the altitude of constant CH_4 mixing ratios. By using CH_4 profiles for the Antarctic fall and spring of 1992, S95 further estimated the middle stratospheric descent over the winter season to be about 1.5–1.8 km month^{-1}.

Before satellite data provided the global distribution of trace gases, we had no direct information on the mean Lagrange circulation in the stratosphere, and it had been studied through indirect frameworks. Recently, *Rosenfield et al.* [1994] used a radiative transfer model to quantify the extent of diabatic descent within the polar vortex; their estimation is consistent with that of S95. *Rosenlof* [1995] studied the residual mean circulation and transport of mass in the stratosphere based on the transformed Eulerian-mean (TEM) equation. It was indicated that the net upward mass flux across a pressure surface (70 hPa) over the equatorial region is larger in the Northern Hemisphere (NH) winter than summer. Another method is described by *Rosenlof and Holton* [1993], who applied the downward control principal proposed by *Haynes et al.* [1991].

S95 gave a reliable estimation of the vertical descent rate within the Antarctic polar vortex using the trace gas, but the estimation was based on an observation for only one winter. The HALOE has continued measuring tracer fields, and now the data record is long enough to see year-to-year variation of the descent rate. Here we will analyze the HALOE data for the period of 1992–1997 using the same method as S95, paying special attention to the average descent rate during the Antarctic fall to spring and its interannual variability. We will also discuss the relationship to the stratospheric circulation.

Because the HALOE measurement reaches high latitudes only twice in a single winter, we can only estimate the "average" descent rate over the winter season. As for the intraseasonal variation in vertical descent, *Rosenfield et al.* [1994] computed diabatic descent within the vortex using a radiative transfer model and showed that during the winter season the descent rate is almost uniform in the middle and lower stratosphere. Further, *Randel et al.* [1998] indicated that CH_4 isolines 0.3–0.8 ppmv at equivalent latitude 76°S move down at an almost constant rate over the winter season based on the analyses of the data from the HALOE and the Cryogenic Limb Array Etalon Spectrometer (CLAES), which provided more continuous sampling of the polar region (about every other month) from January 1992 to April 1993. The equivalent latitude represents a latitude coordinate organized according to potential vorticity fields [*Butchart and Remsberg*, 1986].

This paper is organized as follows: In section 2 we will

Paper number 2000JD900076.
0148-0227/00/2000JD900076$09.00

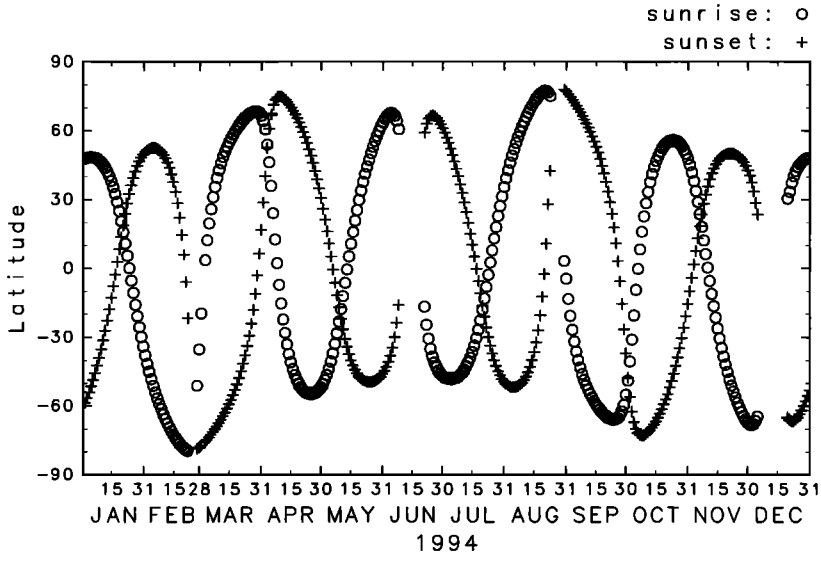

Figure 1. Latitude coverage of the Halogen Occultation Experiment (HALOE) observations for 1994.

describe the HALOE data and the United Kingdom Meteorological Office (UKMO) data that are used to analyze the stratospheric circulation. In section 3 we will introduce an analysis method used by S95 and estimate the descent rate for the six winters. In section 4 we will discuss variations of the descent rate in relation to the stratospheric circulation. Summary and discussion are given in section 5.

2. Data

2.1. HALOE

In this study we use the CH_4 data provided by the HALOE instrument on board the UARS. The HALOE has measured atmospheric chemical constitutes and aerosols using the solar occultation technique since September 1991 [*Russell et al.*, 1993b]. Validation of the HALOE CH_4 data is discussed by *Park et al.* [1996]. We use the version 18 (V18) HALOE data. Differences have been reported between V18 and the latest version (V19). V19 CH_4 sunrise data are larger than those of V18 in the lower stratosphere (by a difference of approximately 5%), but it is not likely to affect the analysis in this study (E. Remsberg, personal communication, 1999). On the other hand, the differences between V16 data that were used by S95 and the V18 data were more significant, because the vertical registration of the profiles was improved for V18. However, we confirmed that V18 CH_4 profiles are quite similar to V16 profiles in the Antarctic polar vortex, and our estimation for 1992 is almost the same as that of S95.

The data (level 2) are available at pressure levels ($1000 \times 10^{-(i-1)/30}$ hPa, $i = 1, 2, \ldots$) for the corresponding height range of 15–75 km, with a vertical spacing of about 0.5 km. Each day, the HALOE obtains 15 sunrise and 15 sunset measurements, each near the same latitude but spaced about 24° apart in longitude. Latitude coverage is from 80°S to 80°N over the course of 1 year (Figure 1). Observations are performed with almost the same latitude progression for each year, but there are slight changes in time and latitude location. Figure 2 indicates the latitude progression of HALOE measurements for each of the six springs (September and October). From 1992 to 1997 the period of high-latitude observations shifts about 3 weeks earlier, and the highest latitude that the HALOE can reach shifts from 78°S to 67°S. Owing to such shifts in latitude and limited spacecraft power, we could get only 50 profiles inside the vortex for the spring of 1997. The number of

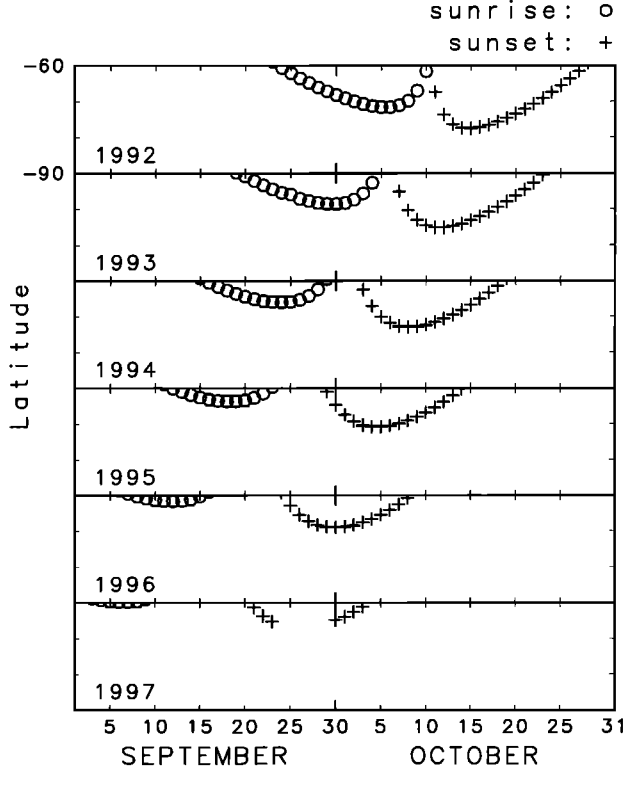

Figure 2. Latitude coverage during September and October from 60°S to 90°S for the 6 years.

profiles for 1997 is about one third compared with that for the other years.

2.2. UKMO

To analyze meteorological fields, we use the UKMO assimilation data [*Swinbank and O'Neill*, 1994]. The globally analyzed fields are mapped on a 2.5° × 3.75° latitude-longitude grid at 22 standard UARS pressure levels spanning 1000–0.3 hPa, with a vertical spacing of about 2.7 km.

Using the UKMO data, Ertel's potential vorticity (PV) is calculated on isentropic surfaces. In a manner similar to S95, we define the latitude with the maximum gradient in a PV field as the vortex boundary (section 3). There is another definition of the vortex boundary based on maximum wind speed [e.g., *Pierce et al.*, 1994], but differences between the two definitions are small in the lower stratosphere, because the maximum PV gradient coincides well with the maximum wind speed.

In section 4 we use the UKMO data arranged in the form of a zonal mean value and zonal Fourier coefficients (wavenumber 1–6) to investigate planetary wave activity. As a measure of wave activity, we calculate the Eliassen-Palm (E-P) flux based on a set of the quasi-geostrophic TEM equations [*Andrews et al.*, 1987]. The residual circulation can be defined by

$$\overline{v^*} \equiv \bar{v} - \rho_0^{-1}(\rho_0 \overline{v'\theta'}/\theta_z)_z, \quad \overline{w^*} \equiv \bar{w} + (\overline{v'\theta'}/\theta_z)_y. \qquad (1)$$

Standard notations are used here [see *Andrews et al.*, 1987]. This describes the Lagrange-mean circulation when the waves are steady and conservative. The zonal mean momentum equation in this case is given by

$$\bar{u}_t - f_0\overline{v^*} - \bar{X} = \rho_0^{-1}\nabla \cdot \mathbf{F} \equiv D_F. \qquad (2)$$

For the case of planetary waves, E-P flux and its divergence are defined as follows:

$$\mathbf{F} \equiv (-\rho_0 \overline{u'v'},\ \rho_0 f_0 \overline{v'\theta'}/\theta_z), \qquad (3)$$

$$\nabla \cdot \mathbf{F} \equiv -(\rho_0 \overline{u'v'})_y + (\rho_0 f_0 \overline{v'\theta'}/\theta_z)_z. \qquad (4)$$

We follow *Shiotani and Hirota* [1985] for the calculation methods.

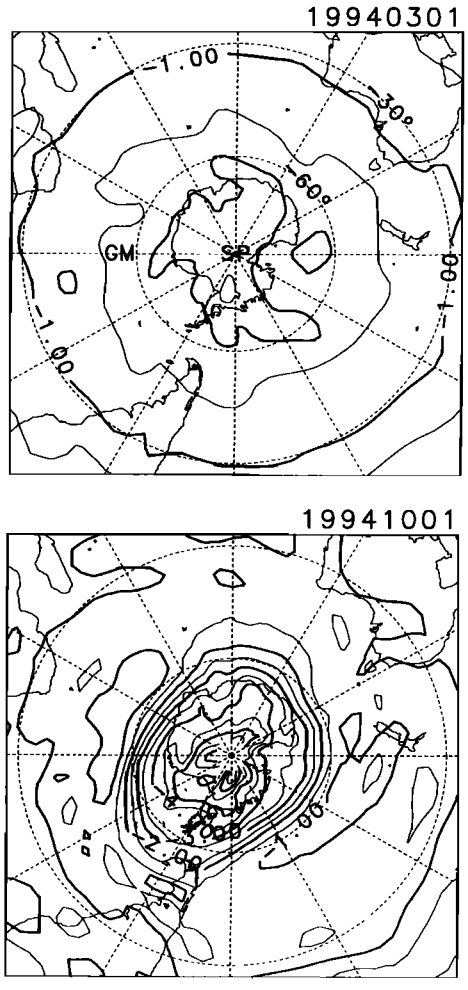

Figure 3. Polar stereographic maps of potential vorticity (PV) on the 750-K isentropic surface (~30 km) on March 1 and October 1, 1994 (contour interval is 0.5×10^{-4} K m^2 s^{-1} kg^{-1}).

3. Estimate of Net Winter Descent

Figure 3 shows polar stereographic maps of the PV for 1 day in fall and 1 day in spring when the HALOE can observe the Antarctic region. In fall the PV field is very flat and the polar vortex is not established yet, but in spring, there are the steep gradients in PV at ~60°S. Over the winter season the polar vortex develops gradually because of the diabatic cooling process and the planetary wave breaking. In the Southern Hemisphere (SH) the polar vortex can remain until late winter because large-scale wave events, like the stratospheric sudden warmings in the NH, rarely occur.

The CH_4 mixing ratio of the air that enters into the stratosphere from the equatorial tropopause decreases with height because of the CH_4 oxidation [*Brasseur and Solomon*, 1986]. Since the lifetime of CH_4 is several years in the middle and lower stratosphere, its distribution is mainly determined by dynamical processes.

Figure 4 shows the relationship between PV and CH_4 for spring observations. There are positive correlations that include a feature caused by the existence of the polar vortex. In 1994, for example, if we compare Figure 3 with Figure 4, the CH_4 mixing ratio inside the polar vortex should be quite different from the outside. Within the polar vortex (less than ~−3 at the PV axis), CH_4 mixing ratios are ~0.3 ppmv, while those outside the vortex (more than ~−1.5 at the PV axis) are larger than 1 ppmv. We confirmed that a similar feature is repeatedly seen for all of the years. The large difference of the mixing ratio inside and outside the vortex agrees with the results of recent satellite measurements and aircraft observations [S95; *Bithell et al.*, 1994; *Proffitt et al.*, 1989; *Kelly et al.*, 1989]. This feature infers that the air inside the polar vortex is highly isolated from the air outside the polar vortex.

Figure 5a shows all CH_4 vertical profiles observed at high latitudes (>60°S) during the spring observation (September and October). In the middle and lower stratosphere, profiles are separated into two groups, as already described in Figure 4: The CH_4 mixing ratio is small inside the vortex and large outside the vortex. Inside the vortex the mixing ratio decreases with height from the lower to middle stratosphere, and it has a local minimum around the middle stratosphere (~10 hPa). At this level it is confirmed that profiles within the vortex always have values less than ~0.3 ppmv (see also Figure 4). On the other hand, above the middle stratosphere, the mixing ratio is

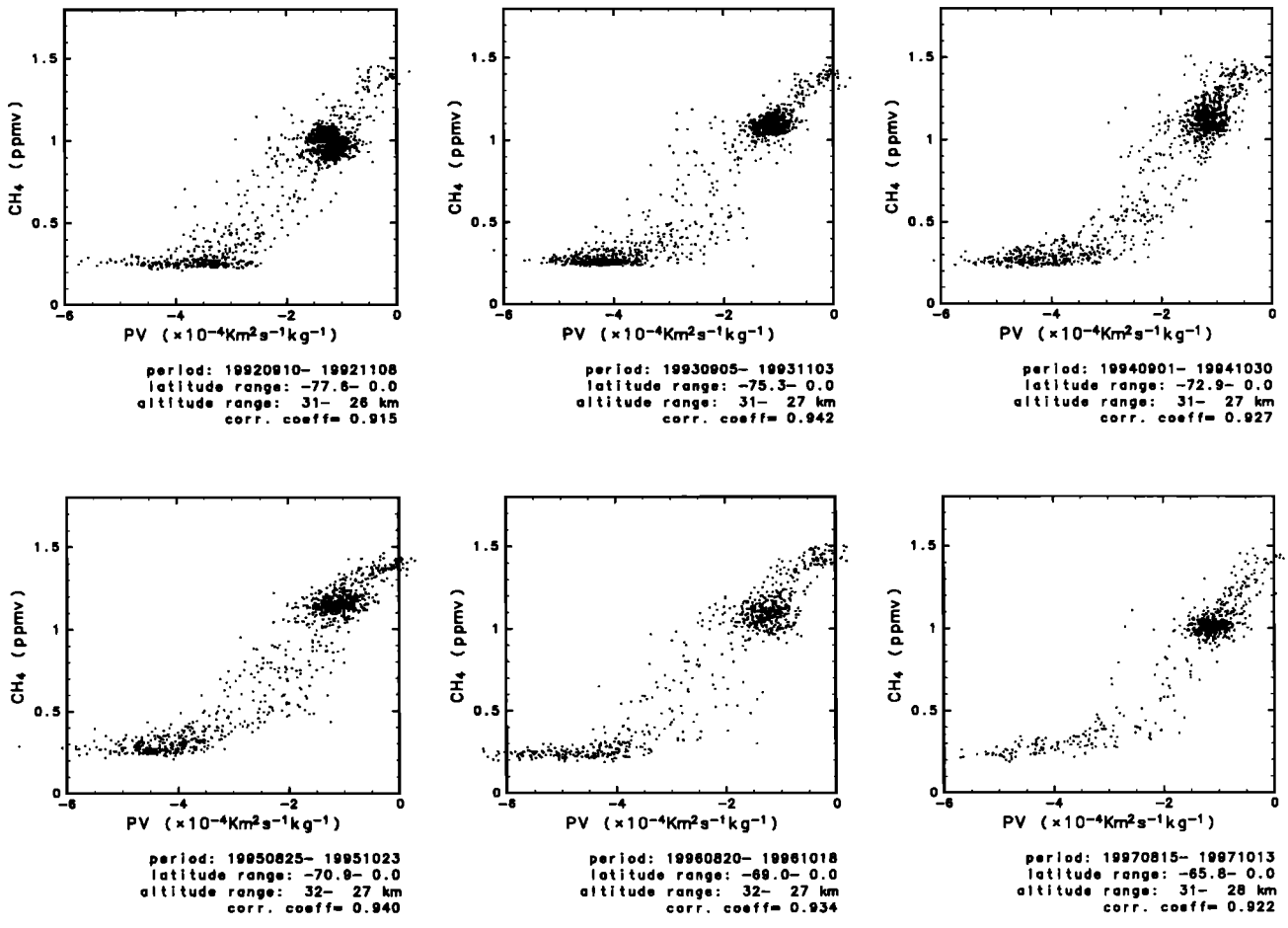

Figure 4. Plots of CH_4 versus PV on the 750-K isentropic surface for the six springs.

almost constant or increases over the upper stratosphere. Thus, on the basis of the CH_4 mixing ratio on a midstratospheric pressure level where CH_4 has a local minimum (hereinafter referred to as a reference pressure level), we define profiles which have values less than 0.3 ppmv as those inside the polar vortex. We have investigated CH_4 profiles for six springs and confirmed that the CH_4 mixing ratio inside the vortex is always less than 0.3 ppmv at each reference pressure level in the middle stratosphere. In this study we used the following reference pressure levels to distinguish the profiles: 1992, 21.5 hPa; 1993, 14.7 hPa; 1994–1996, 12.6 hPa; and 1997, 11.7 hPa. The reference pressure level for 1992 is the same as that for S95. We note that the estimation of the vertical descent rate is not affected by the location of the reference pressure level, if profiles inside the vortex are clearly distinguishable from those outside.

The spring profiles within the polar vortex and all of the fall profiles in 1994 are shown in Figure 5b. The fall profiles do not separate because the polar vortex does not exist. The spring profiles show some variability up to 50 km because of large off-polar displacement of the polar vortex (S95). From fall to spring (about 7 months) the slope of CH_4 values 0.3–0.9 ppmv moves down about 10 km. If the air follows the vertical mass flow in the polar vortex, net descent over the winter season can be estimated from the difference of the two slopes.

Figure 6 shows the average profiles for fall and spring for each of the 6 years. During the spring of 1992 the off-polar displacement is particularly large because of vigorous planetary wave activity (see section 4 and Figure 8c). Figure 6 shows another important difference: Altitudes of the slopes of 0.3–0.9 ppmv for the 6 years change slightly from year to year. For the fall profiles, most of the slopes of 1992, 1994, and 1996 (dashed lines in Figure 6) are located at higher altitudes than those of 1993, 1995, and 1997 (solid lines). This suggests that interannual variations are already present in early winter. The slopes among the solid and dashed lines shift to successively higher altitudes year by year. This seems to correspond to the time shift of the HALOE measurements shown in Figure 2: If the descent has already begun by this time of year and the descent rate is about 1.5 km $month^{-1}$ (see next paragraph), the slopes shift upward about 0.2 km annually. This is because high-latitude observations were performed about 4 days earlier every year as time progressed. On the other hand, the spring profiles simply move up every year (~1 km yr^{-1}). Because this rate is larger than that caused by the time shift of the observation, the descent rate is expected to display a decreasing trend; but this upward movement of the spring slopes is probably enhanced to some extent by the latitudinal movement of the HALOE observation mentioned in section 2. Since the HALOE spring observations move farther away from the Antarctic pole every year, there is an annual increase in the ratio of profiles near the vortex edge to all profiles that are defined

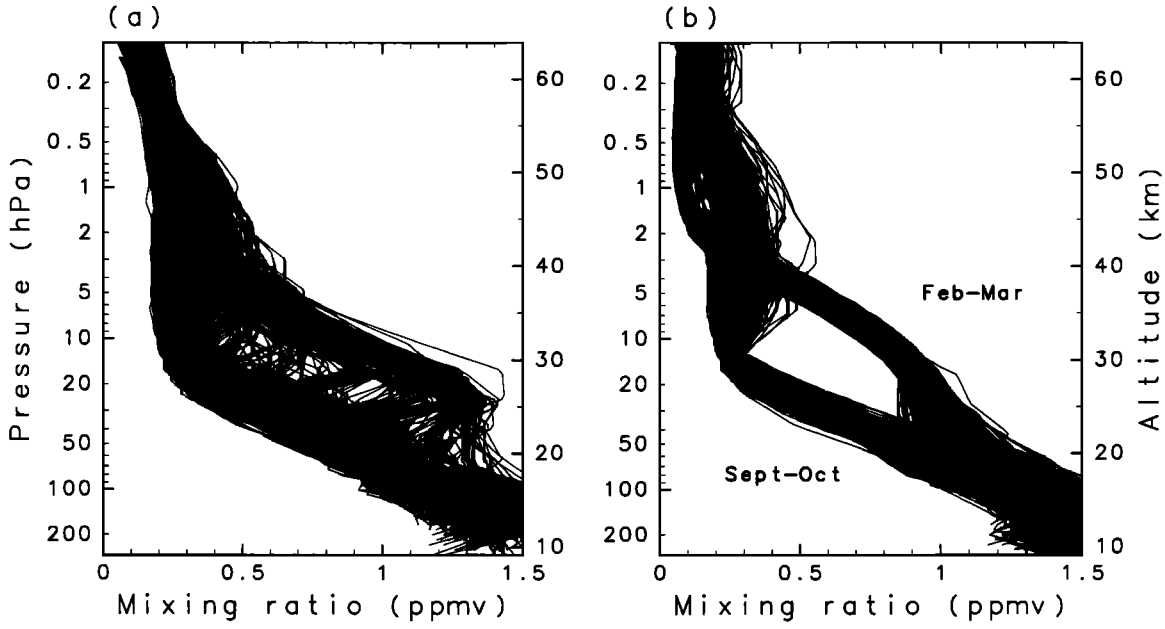

Figure 5. (a) All of the CH_4 vertical profiles in the polar region (>60°S) during September and October, 1994. (b) Upper lines indicate profiles during February and March, 1994 (>60°S). Lower lines indicate profiles inside the polar vortex during September and October, 1994 (>60°S).

as those within the vortex. Because profiles near the edge have slightly larger mixing ratios than those over the vortex center, spring slopes are likely to be located at higher altitudes every year. However, we consider that the effect from this is small in our study, because HALOE has obtained enough profiles within the vortex for all the years excluding 1997.

Figure 7 shows the vertical descent rates at 0.3, 0.4, 0.5, 0.6, 0.7, 0.8, and 0.9 ppmv for each of the six winters estimated from the differences between fall and spring profiles. These are within the range of about 1.1–1.9 km $month^{-1}$. By incorporating these values into the TEM thermodynamic equation, we can calculate an average net heating rate from February to October. It is estimated at -0.45 to -0.65 K d^{-1} when the air having a CH_4 mixing ratio of 0.6 ppmv moves from ~35 to ~25 km (around 10 hPa) and the temperature profile at 10 hPa for

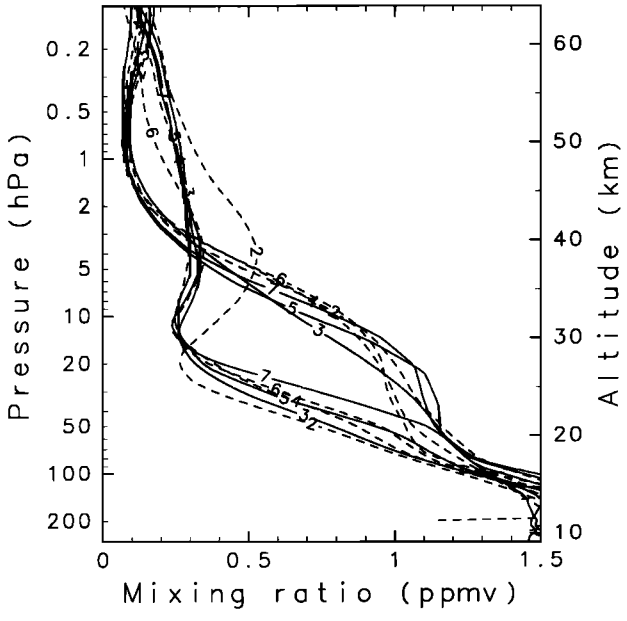

Figure 6. Same as Figure 5b, but for the average CH_4 vertical profiles for the 6 years. Dashed and solid lines indicate the even and odd years, respectively. The numbers on the lines indicate the last numeral of the year it represents (for example, "2" means 1992).

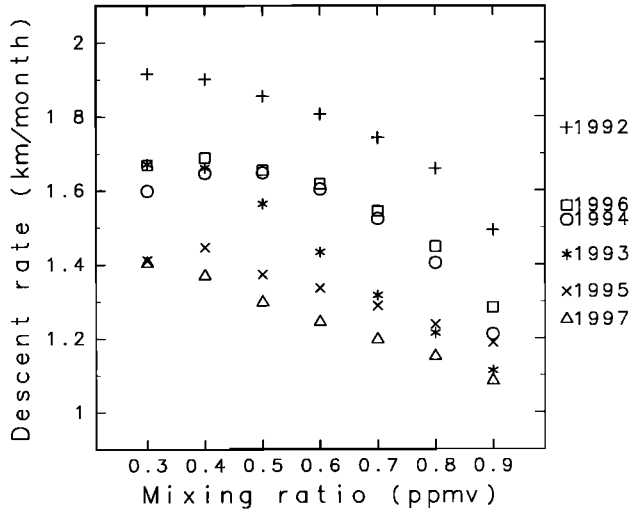

Figure 7. Average winter descent rates from fall to spring for each mixing ratio (0.3–0.9 ppmv). Values on the right axis are averages from 0.3 to 0.9 ppmv. Error bars (at 0.6 ppmv) for each year are indicated in Figure 9, because they have almost the same values in the range of 0.3–0.9 ppmv.

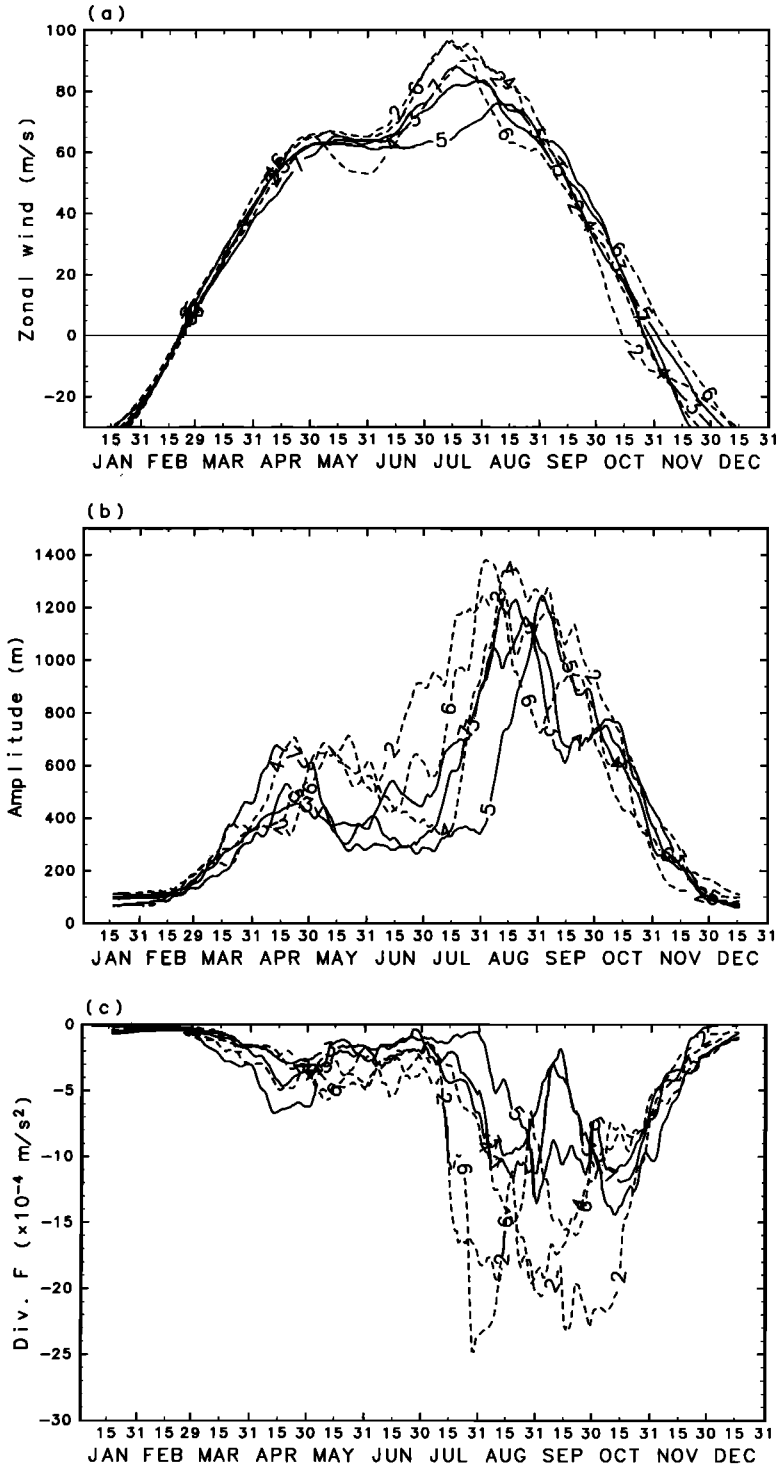

Figure 8. (a) Zonal mean zonal wind at 1 hPa and 60°S. Dashed and solid lines indicate the even and odd years, respectively. A 31-day running mean is applied to Figures 8a, 8b, and 8c. (b) Amplitudes of geopotential height of the zonal wavenumber 1 component at 1 hPa and 60°S. (c) Eliassen-Palm (E-P) flux divergence of the zonal wavenumber 1 component at 1 hPa and 60°S.

80°–90°S is used. For winter 1992, *Rosenfield et al.* [1994] calculated a vortex-averaged heating rate to be about -1 K d^{-1} on the 800-K isentropic surface (~10 hPa) from March to October. Their heating rate is somewhat larger than our estimation for 1992 (~-0.6 K d^{-1}).

In Figure 7 we can see two variations. First, the descent rates are larger at lower mixing ratios, that is, at higher altitudes. If we assume that $v_y^* \sim 0$ in the continuity equation, since the Antarctic polar vortex seems to be highly isolated, we obtain the relationship $w^*(z) \propto e^{z/H}$ (H is scale height). The descent

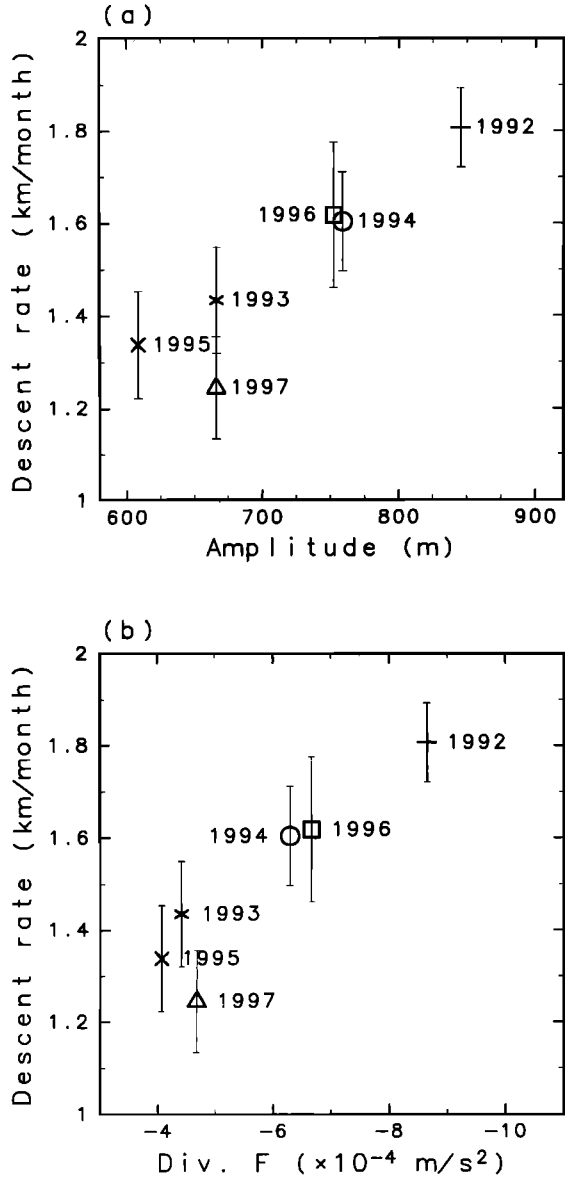

Figure 9. (a) Descent rate at 0.6 ppmv versus geopotential height amplitude of the zonal wave number 1 component at 1 hPa and 60°S averaged from February to October. Error bars (at 0.6 ppmv) are estimated by a deviation (1σ) of spring profiles within the polar vortex. (b) Descent rate versus E-P flux divergence of the zonal wavenumber 1 component at 1 hPa and 60°S.

rate is expected to be large in upper levels. Since the difference of average altitudes between 0.4 and 0.8 ppmv is about 5 km, the descent rate for 0.4 ppmv needs to be about twice as large as that for 0.8 ppmv. However, Figure 7 indicates that the descent rates for 0.4 and 0.8 ppmv differ only by a factor of ~1.2 (average of the 6 years). One of the most likely reasons for this disagreement is due to the assumption of vortex isolation. In the SH the polar vortex is generally highly isolated from the air of the midlatitudes, because a region of steep radial PV gradients acts as a very effective barrier to cross-vortex mass exchange [e.g., *Chen et al.*, 1994; *Chen*, 1994]. On the other hand, the existence of mass flow through the vortex edge has been reported [e.g., *Rosenlof et al.*, 1997]. The disagreement we observed may be caused by such mass flow through the vortex edge.

The second point we should stress concerns interannual variability. Figure 7 shows that the descent rates have large year-to-year variations (1.2–1.8 km month^{-1} at 0.6 ppmv). Moreover, they display biennial oscillations and decreasing trends. In the next section we will investigate the variation in relation to the stratospheric circulations.

4. Relation to the Stratospheric Circulations

The stratospheric circulations of the two hemispheres differ in many aspects. One of the most characteristic features of the SH circulation is a poleward and downward movement of the polar night jet during midwinter [e.g., *Hartmann et al.*, 1984]. This movement occurs at different times in different years [*Mechoso et al.*, 1985; *Shiotani and Hirota*, 1985]. In addition, amplitudes of the planetary waves are small in midwinter and show two peaks in early and late winter [*Hirota et al.*, 1983]. It is also known that the active period of planetary waves is related to the time of the movement of the westerly jet [*Shiotani et al.*, 1993].

Figure 8a shows the seasonal march of zonal mean zonal wind at 1 hPa and 60°S. The profiles have two peaks, a small one in late April and another in July or August. The second peak is stronger and shows larger year-to-year variability. In 1992 and 1996 the second peak reaches ~90 m s^{-1} at mid-July, while in 1995 it is weak (~70 m s^{-1}) and occurs in mid-August. On the whole, the second peak is stronger and occurs earlier in the even years (dashed lines in Figure 8) than in the odd years (solid lines). This result suggests that the time of the poleward and downward movement of the westerly jet is earlier in the even years. Such variability in the zonal wind is likely related to that in planetary wave activity because the planetary wave and zonal mean flow interact with each other.

Figure 8b shows the seasonal march of zonal wavenumber 1 amplitudes of the geopotential height field. Two seasons of vigorous wave activities are seen in early and late winter. Moreover, in the odd years the first maximum appears earlier (April), but the second maximum appears later (mid-August to early September) than in the even years. When the amplitude increases toward the second maximum, the zonal wind becomes stronger, as seen from comparison of Figures 8a and 8b. These features of the planetary wave amplitude in the even and odd years are quite similar to those indicated by *Shiotani et al.* [1993] in which the SH winter circulation is classified into two categories during the 1980s, depending on the location of the westerly jet in July and in the upper stratosphere (1 hPa): high-latitude-jet (HLJ) year, with maximum westerlies around 50°S, low-latitude-jet (LLJ) year, with maximum westerlies around 40°S. The even and odd years correspond to HLJ and LLJ, respectively, although the average latitudes of the even and odd years in July are located rather poleward (55°S and 45°S, respectively; see Figure 10). *Shiotani et al.* [1993] argued that once the maximum westerlies are established at high latitudes during midwinter, the E-P vectors, which are measures of wave activity, are effectively guided up into higher latitudes. Therefore the active period of the planetary wave appears when the poleward and downward movement of the westerly jet occurs. This feature is also seen in Figure 8c. The E-P flux convergence becomes large in correspondence to the movement of the westerly jet, and after the movement of the westerly jet, the increased wave activity remains until late winter.

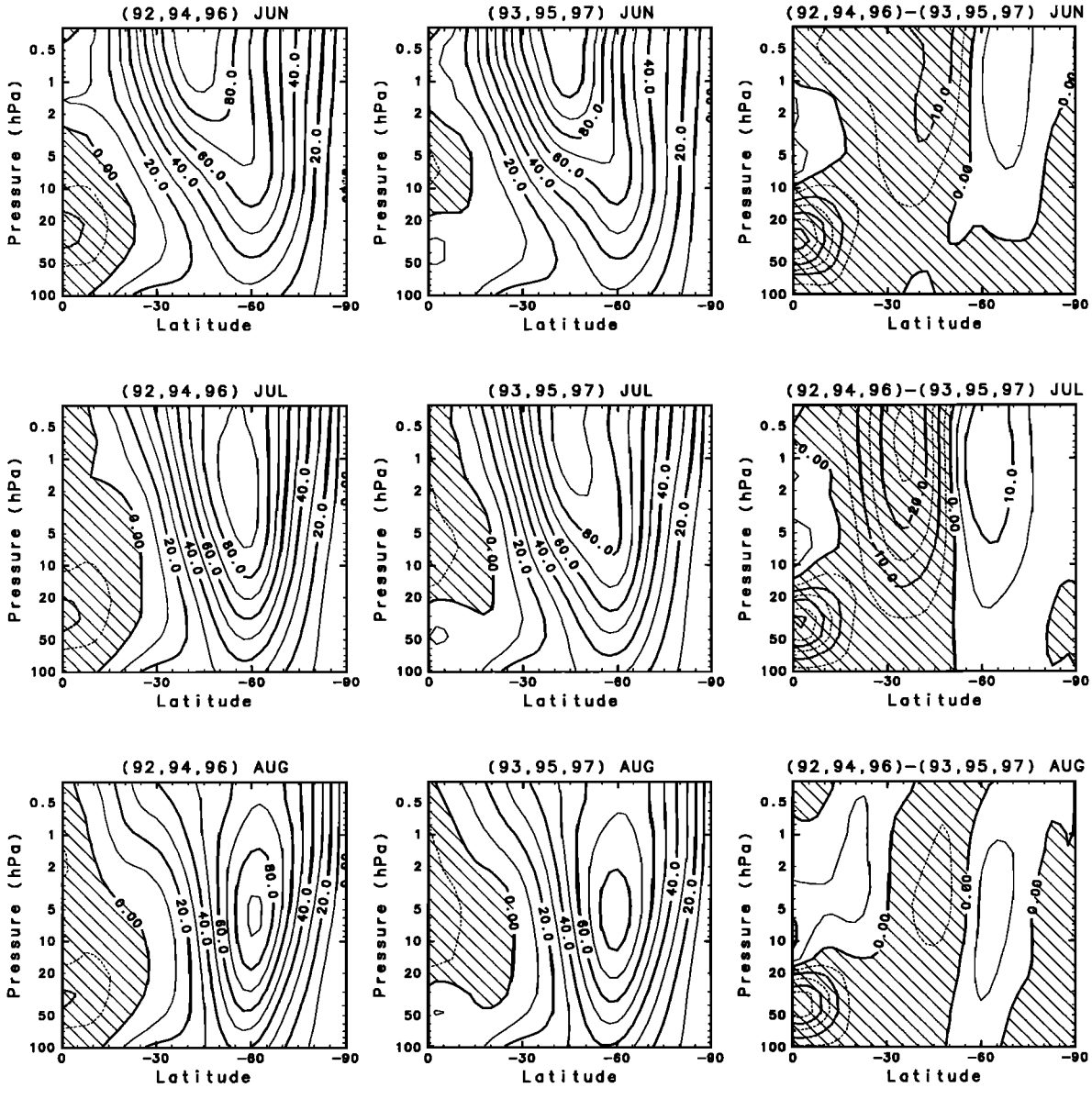

Figure 10. Latitude-height section of monthly-mean composite zonal mean zonal wind in June, July, and August. Left column shows 1992, 1994, and 1996; middle column shows 1993, 1995, and 1997; and right column shows the differences between the even and odd years (contour interval is 10 m s^{-1} for left and middle columns and 5 m s^{-1} for right column; negative values are shown hatched).

Thus the planetary wave activity during midwinter to late winter is more vigorous in the even years than in the odd years.

As shown in Figures 8b and 8c, planetary wave activities tend to be larger in the even years, that is, in 1992, 1994, and 1996, when the descent rates are larger. We attempted to show the relationship between the descent rate and planetary wave activity and found that the two show a good positive correlation (Figure 9a). The descent rate is larger for years with larger amplitudes of the planetary-scale waves (in this case, wavenumber 1 component) over the winter season. This relation holds at high latitudes from the middle to upper stratosphere. We have also confirmed a similar relationship using D_F (Figure 9b). Descent rates are larger in years with large convergence of D_F at the upper stratosphere (1 hPa, 60°S), where strong convergence can be seen over the winter. The above two relations (Figures 9a and 9b) are retained in the total wavenumber fields constructed from zonal wavenumber 1–6 components. Here we notice that the amplitude and D_F also have decreasing trends corresponding to the descent rate. Thus the decreasing trend seen in the descent rate seems to be related to a trend of the SH stratospheric circulations.

Here we briefly mention the winter of 1997, when the values do not follow the relationships displayed in Figure 9. In the SH stratospheric winter it is known that zonal wavenumber 1 component of planetary waves is quasi-stationary. In 1997, however, traveling waves are dominant, and they account for a large part of the total amplitudes. After removing the traveling wave component, the amplitude of 1997 moves closer to the

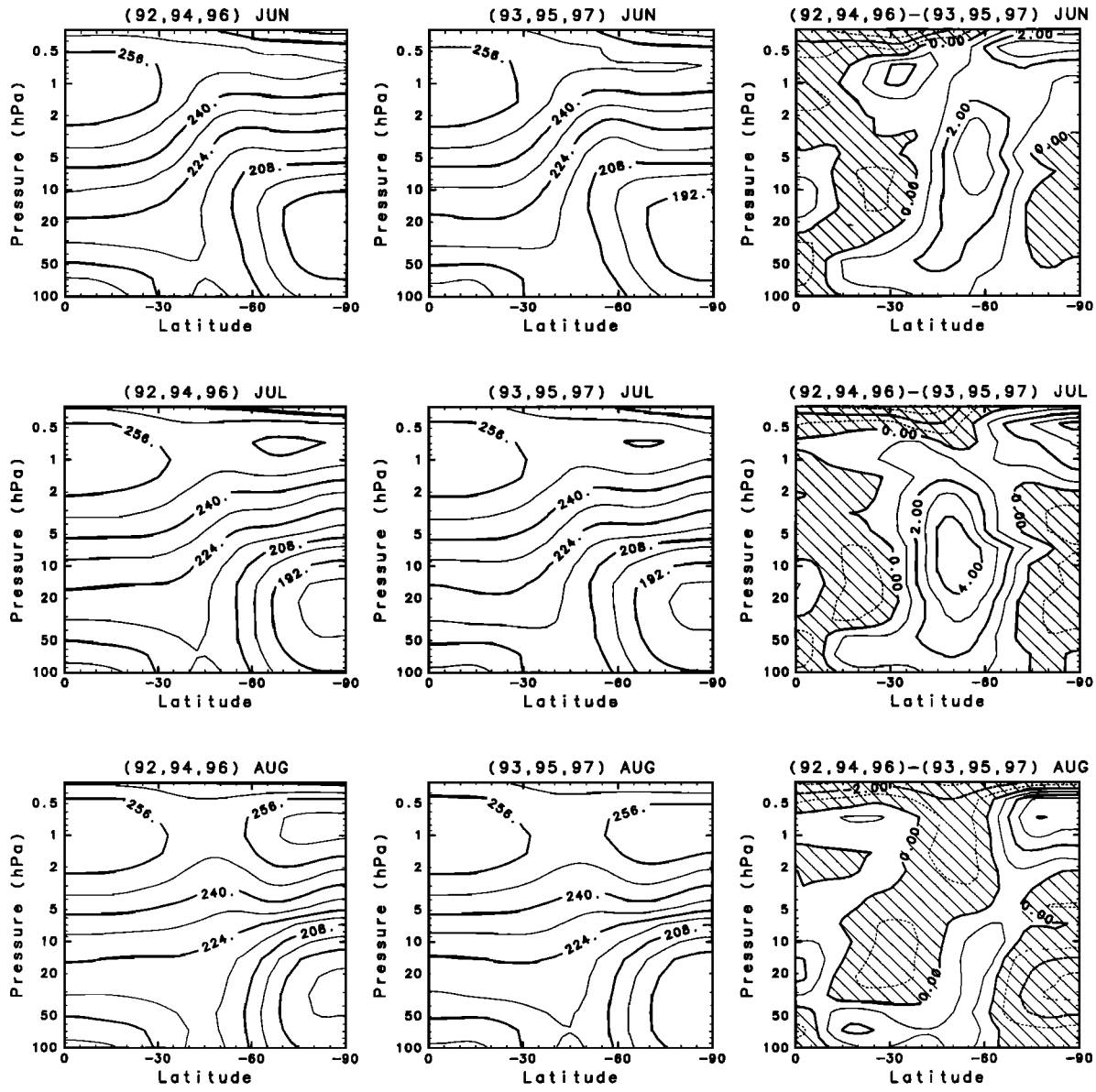

Figure 11. Same as Figure 10, but for temperature fields (contour interval is 8 K for left and middle columns and 1 K for right column; negative values are shown hatched).

line of the other years. We expect a good correlation between the descent rate and planetary-scale stationary waves.

The results so far indicate that the stratospheric circulations differ between the even and odd years for the period 1992–1997. To make the difference clear, we performed a composite analysis for the even and odd years and found that the composite fields show large differences during midwinter. Figure 10 shows composite cross sections and the differences for the zonal mean zonal wind fields in June, July, and August. In both the even and odd years the maximum westerlies in the upper stratosphere move poleward and downward, as reported by *Hartmann et al.* [1984]. The movement occurs earlier, however, in the even years: In July, the maximum westerly lies at 60°S and 2 hPa in the even years, while it lies at 40°S and the lower mesosphere in the odd years. The difference shows a dipole pattern with a nodal latitude around 50°S, which is remarkable in July (right column in Figure 10). In Figure 10, another difference is seen over the equator in relation to the equatorial quasi-biennial oscillation (QBO). Discussion about the QBO is given in section 5.

The composite temperature fields also indicate many interesting features corresponding to the zonal wind fields as a result of the thermal wind relation (Figure 11). When the westerly jet moves poleward and downward, the meridional gradient around the latitude range 40°–50°S in the middle and upper stratosphere becomes weak, and the temperature around the Antarctic stratopause (~1 hPa) rises. This warm Antarctic stratopause is known as a "warm pool," where high temperatures are maintained against the radiative equilibrium. Because solar heating is not expected over the midwinter polar region, one of the most likely causes for this is adiabatic heating with downwelling motion [*Hitchman et al.*, 1989]. When the downwelling motion is dominant, adiabatic heating is large and the temperature should be kept high. This scenario agrees with our results: The Antarctic stratopause is warmer in the even years with larger descent rates. The larger adiabatic heating

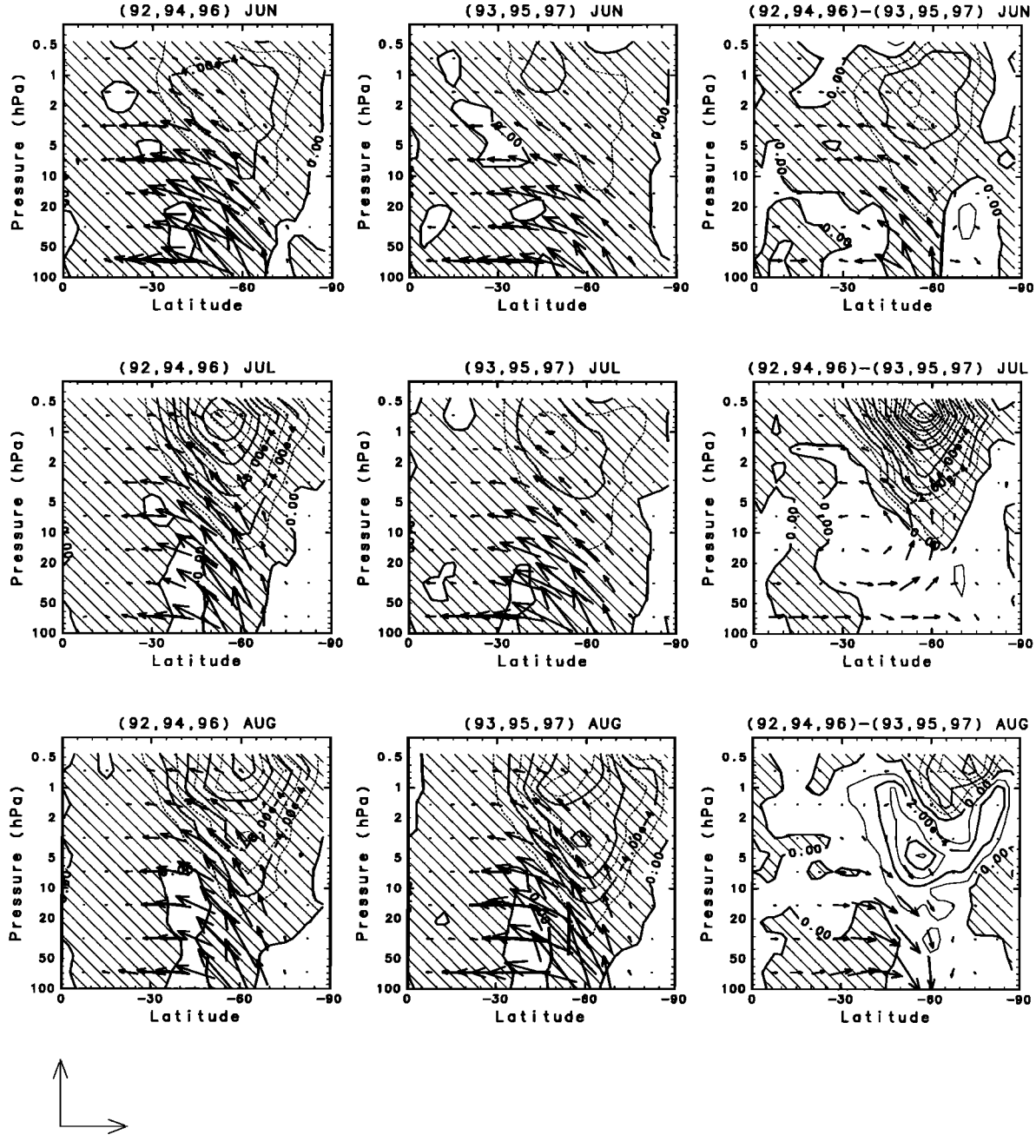

Figure 12. Same as Figure 10, but for the E-P flux vector and its divergence (contour interval is 2.0×10^{-4} m s^{-2} for left and middle columns and 1.0×10^{-4} m s^{-2} for right column; negative values are shown hatched). The length of the unit vectors corresponds to 5.0×10^{6} kg s^{-2} for the horizontal component and $c \times 5.0 \times 10^{6}$ kg s^{-2} for the vertical component ($c = 125$).

with larger descent motion in the even years warms up the Antarctic stratopause effectively. On the other hand, the middle to lower stratosphere is cooler in the even years than in the odd years, strongly reflecting the distribution of the zonal wind field. In September, however, all altitudes of the Antarctic become warmer in the even years.

As discussed in Figure 8, the movement of the maximum westerlies is also related to the propagation of the planetary waves because the planetary wave and mean flow interact with each other. Figure 12 shows composite E-P vectors and their divergence fields. The E-P vectors originating from the troposphere point equatorward and upward in the stratosphere. After the movement of maximum westerlies, the E-P vectors turn remarkably upward. This occurs in July in the even years and in August in the odd years. Corresponding to the increase in the upward propagation, the convergence at high latitudes and upper stratosphere becomes large.

5. Summary and Discussion

The long-lived atmospheric minor gas CH_4 data observed by the HALOE have been used to estimate a vertical descent rate

in the Antarctic polar vortex. Using an analysis technique similar to that of S95, we calculated average descent rates over the winter seasons for each of the 6 years from 1992 to 1997. The descent rate is in the range of 1.1–1.9 km month^{-1} for CH_4 mixing ratios in the range 0.3–0.9 ppmv.

The descent rates show interesting large year-to-year variations (1.2–1.8 km month^{-1} at 0.6 ppmv), which include the biennial oscillation and the decreasing trend for the period we analyzed. The descent rate is larger in 1992, 1994, and 1996 than in 1993, 1995, and 1997. Thus we investigated the variation in relation to the stratospheric circulations. Differences between the even and odd years in the meteorological fields are remarkable during the midwinter. In the even years a downward and poleward movement of the westerly jet occurs earlier. The movement is associated with the development of a warm pool around the Antarctic stratopause because the zonal wind distribution is related to the temperature distribution through the thermal wind relation. Our result showed that the temperature around the Antarctic stratopause rises earlier in the even years, probably because of the larger adiabatic heating with the larger descent motion. The movement of the westerly jet is also related to an earlier enhancement of planetary wave activities in the even years. Therefore the descent rate and planetary wave activity have a positive correlation.

We mentioned that the seasonal evolutions of planetary wave amplitudes in the even and odd years are quite similar to those of the two types classified by *Shiotani et al.* [1993]; the even and odd years correspond to HLJ and LLJ years, respectively. *Shiotani et al.* [1993] pointed out that the seasonal march of the SH circulation is already decided in early winter (see Figure 8b). When the first maximum of planetary wave amplitudes appears later, it is expected that the second maximum and the movement of the westerly jet occur earlier. It is interesting that fall CH_4 profiles also show a year-to-year variation corresponding to the stratospheric circulation: The fall CH_4 profiles are located at higher altitudes in the even years than in the odd years (Figure 6). This result indicates that early winter variability in dynamical fields also reflects the long-lived chemical gas distributions.

In Figure 10 we see another variation over the equator. This corresponds to the QBO. In this study the descent rate is larger in the even years when the equatorial zonal flow is in the easterly phase of the QBO. In the NH the QBO influence on winter circulation has been investigated in detail [e.g., *Holton and Tan*, 1980]. When the QBO is in the easterly phase, the northern polar vortex tends to be highly disturbed by waves and resulting sudden warmings. Such clear relationships have not been reported for the SH, but our result indicates that planetary waves are active in the QBO easterly years during the period 1992–1997 (section 4). This feature is consistent with that of the NH. On the other hand, it is reported that QBO-synchronized variations in the minimum temperature (~100 hPa) and in the column ozone occurred within the spring Antarctic polar vortex during the 1980s [*Garcia and Solomon*, 1987; *Lait et al.*, 1989; *Randel and Cobb*, 1994]. In October the temperature is higher and the ozone is richer in the QBO easterly years than in the QBO westerly years. We also investigated the temperature in October for 1992–1997 and found that the minimum temperature shows the year-to-year synchronization with the QBO. Moreover, the minimum temperature is in good positive correlation with the descent rate.

Finally, we discuss the relationship between the QBO and the interannual variability of the stratospheric westerly jet location in midwinter. During 1992–1997 the westerly jet in the midwinter is located at higher latitudes when the equatorial zonal flow is in the easterly phase of the QBO. On the other hand, the replacement of HLJ and LLJ in the 1980s does not have the QBO periodicity. Recently, *Kuroda and Kodera* [1998] indicated that the dipole pattern, as depicted in Figure 10 of the present paper, is distinguished in the empirical orthogonal function analysis of the zonal wind fields for the period 1979–1994. The time coefficients of this mode exhibit a clear biennial oscillation, that is, the westerly jet replacement occurs with a period of 2 years. On the basis of these reports and our results, it is certain that interannual variability exists with a period of about 2 years in the SH winter circulation, though the relationship to the QBO and so on are not clear.

Acknowledgments. Special thanks are given to the HALOE science team for providing the HALOE data. We retrieved HALOE data and the necessary information from the HALOE home page. Further information about HALOE methane data was provided by Ellis E. Remsberg of the NASA Langley Research Center. The authors are also grateful to the U.K. Meteorological Office for providing the data sets and to Hiroo Hayashi for handling the UKMO data. We thank James M. Russell III, Hiroshi Kanzawa, Shigeo Yoden, and three anonymous reviewers for their helpful comments and suggestions. The GFD-DENNOU Library was used for drawing the figures.

References

Andrews, D. G., J. R. Holton, and C. B. Leovy, *Middle Atmosphere Dynamics*, 498 pp., Academic, San Diego, Calif., 1987.

Bithell, M., L. J. Gray, J. E. Harries, J. M. Russell III, and A. F. Tuck, Synoptic interpretation of measurements from HALOE, *J. Atmos. Sci.*, *51*, 2942–2956, 1994.

Brasseur, G., and S. Solomon, *Aeronomy of the Middle Atmosphere: Chemistry and Physics in the Stratosphere and Mesosphere*, 2nd ed., 452 pp., D. Reidel, Norwell, Mass., 1986.

Butchart, N., and E. E. Remsberg, The area of the stratospheric polar vortex as a diagnostic for tracer transport on an isentropic surface, *J. Atmos. Sci.*, *43*, 1319–1339, 1986.

Chen, P., The permeability of the Antarctic vortex edge, *J. Geophys. Res.*, *99*, 20,563–20,571, 1994.

Chen, P., J. R. Holton, A. O'Neill, and R. Swinbank, Quasi-horizontal transport and mixing in the Antarctic stratosphere, *J. Geophys. Res.*, *99*, 16,851–16,866, 1994.

Garcia, R. R., and S. Solomon, A possible relationship between interannual variability in Antarctic ozone and the quasi-biennial oscillation, *Geophys. Res. Lett.*, *14*, 848–851, 1987.

Hartmann, D. L., C. R. Mechoso, and K. Yamazaki, Observations of wave-mean flow interaction in the Southern Hemisphere, *J. Atmos. Sci.*, *41*, 351–362, 1984.

Haynes, P. H., C. J. Marks, M. E. McIntyre, T. G. Shepherd, and K. P. Shine, On the "downward control" of extratropical diabatic circulations by eddy-induced mean zonal forces, *J. Atmos. Sci.*, *48*, 651–678, 1991.

Hirota, I., T. Hirooka, and M. Shiotani, Upper stratospheric circulations in the two hemispheres observed by satellites, *Q. J. R. Meteorol. Soc.*, *109*, 443–454, 1983.

Hitchman, M. H., J. C. Gille, C. D. Rodgers, and G. Brasseur, The separated polar winter stratopause: A gravity wave driven climatological feature, *J. Atmos. Sci.*, *46*, 410–422, 1989.

Holton, J. R., and H.-C. Tan, The influences of the equatorial quasi-biennial oscillation on the global circulation at 50 mb, *J. Atmos. Sci.*, *37*, 2200–2208, 1980.

Kelly, K. K., et al., Dehydration in the lower Antarctic stratosphere during late winter and early spring, 1987, *J. Geophys. Res.*, *94*, 11,317–11,357, 1989.

Kuroda, Y., and K. Kodera, Interannual variability in the troposphere and stratosphere of the Southern Hemisphere winter, *J. Geophys. Res.*, *103*, 13,787–13,799, 1998.

Lait, L. R., M. R. Schoeberl, and P. A. Newman, Quasi-biennial mod-

ulation of the Antarctic ozone depletion, *J. Geophys. Res.*, *94*, 11,559–11,571, 1989.

Mechoso, C. R., D. L. Hartmann, and J. D. Farrara, Climatology and interannual variability of wave, mean-flow interaction in the Southern Hemisphere, *J. Atmos. Sci.*, *42*, 2189–2206, 1985.

Park, J. H., et al., Validation of Halogen Occultation Experiment CH_4 measurements from the UARS, *J. Geophys. Res.*, *101*, 10,183–10,203, 1996.

Pierce, R. B., W. L. Grose, J. M. Russell III, and A. F. Tuck, Evolution of Southern Hemisphere spring air masses observed by HALOE, *Geophys. Res. Lett.*, *21*, 213–216, 1994.

Proffitt, M. H., K. K. Kelly, J. A. Powell, B. L. Gary, M. Loewenstein, J. R. Podolske, S. E. Strahan, and K. R. Chan, Evidence for diabatic cooling and poleward transport within and around the 1987 Antarctic ozone hole, *J. Geophys. Res.*, *94*, 16,797–16,813, 1989.

Randel, W. J., and J. B. Cobb, Coherent variations of monthly mean total ozone and lower stratospheric temperature, *J. Geophys. Res.*, *99*, 5433–5447, 1994.

Randel, W. J., F. Wu, J. M. Russell III, A. Roche, and J. W. Waters, Seasonal cycles and QBO variations in stratospheric CH_4 and H_2O observed in UARS HALOE data, *J. Atmos. Sci.*, *55*, 163–185, 1998.

Rosenfield, J. E., P. A. Newman, and M. R. Schoeberl, Computations of diabatic descent in the stratospheric polar vortex, *J. Geophys. Res.*, *99*, 16,677–16,689, 1994.

Rosenlof, K. H., Seasonal cycle of the residual mean meridional circulation in the stratosphere, *J. Geophys. Res.*, *100*, 5173–5191, 1995.

Rosenlof, K. H., and J. R. Holton, Estimates of the stratospheric residual circulation using the downward control principle, *J. Geophys. Res.*, *98*, 10,465–10,479, 1993.

Rosenlof, K., H., A. F. Tuck, K. K. Kelly, J. M. Russell III, and M. P. McCormick, Hemispheric asymmetries in water vapor and inferences about transport in the lower stratosphere, *J. Geophys. Res.*, *102*, 13,213–13,234, 1997.

Russell, J. M., III, A. F. Tuck, L. L. Gordley, J. H. Park, S. R. Drayson, J. E. Harries, R. J. Cicerone, and P. J. Crutzen, HALOE Antarctic observations in the spring of 1991, *Geophys. Res. Lett.*, *20*, 719–722, 1993a.

Russell, J. M., III, L. L. Gordley, J. H. Park, S. R. Drayson, W. D. Hesketh, R. J. Cicerone, A. F. Tuck, J. E. Frederick, J. E. Harries, and P. J. Crutzen, The Halogen Occultation Experiment, *J. Geophys. Res.*, *98*, 10,777–10,797, 1993b.

Schoeberl, M. R., M. Luo, and J. E. Rosenfield, An analysis of the Antarctic Halogen Occultation Experiment trace gas observations, *J. Geophys. Res.*, *100*, 5159–5172, 1995.

Shiotani, M., and I. Hirota, Planetary wave–mean flow interaction in the stratosphere: A comparison between Northern and Southern Hemispheres, *Q. J. R. Meteorol. Soc.*, *111*, 309–334, 1985.

Shiotani, M., N. Shimoda, and I. Hirota, Interannual variability of the stratospheric circulation in the Southern Hemisphere, *Q. J. R. Meteorol. Soc.*, *119*, 531–546, 1993.

Swinbank, R., and A. O'Neill, A stratosphere-troposphere data assimilation system, *Mon. Weather Rev.*, *122*, 686–702, 1994.

N. Kawamoto, Department of Geophysics, Faculty of Science, Kyoto University, Kyoto 606-8502, Japan. (kawamoto@kugi.kyoto-u.ac.jp)

M. Shiotani, Division of Ocean and Atmospheric Sciences, Graduate School of Environmental Earth Science, Hokkaido University, Sapporo 060-0810, Japan.

(Received July 21, 1999; revised January 14, 2000;
accepted January 21, 2000.)